PERGAMON

Chemical Engineering Science 57 (2002) 1531–1536

Chemical
Engineering Science

www.elsevier.com/locate/ces

Gas and liquid phase mass transfer within KATAPAK-S® structures studied using CFD simulations

J. M. van Baten, R. Krishna *

Department of Chemical Engineering, University of Amsterdam, Nieuwe Achtergracht 166, Amsterdam, WV 1018, The Netherlands

---

Abstract

The gas phase mass transfer in the empty channels, and the liquid phase mass transfer within the catalyst-packed channels, of the criss-crossing sandwich structures of KATAPAK-S have been studied using computational fluid dynamics. Due to the “upheaval” caused by the flow splitting at the cross-overs, the mass transfer coefficient is significantly larger than that for fully developed flow in a single tube. © 2002 Elsevier Science Ltd. All rights reserved.

Keywords: Structured packing; Mass transfer; Computational fluid dynamics

---

1. Introduction

For heterogeneously catalysed reactive distillation processes, hardware design poses considerable challenges (Taylor & Krishna, 2000). The catalyst particle sizes used in such operations are usually in the 1–3 mm range. Larger particle sizes lead to intra-particle diffusion limitations. To overcome the limitations of flooding during counter-current vapour-liquid contacting, the catalyst particles have to be enveloped within wire gauze structures. Two commonly used structures in industry are described below.

1. Catalyst particles enclosed in cloth wrapped in the form of bales (Smith Jr., 1985; Johnson & Dallas, 1994; Subawalla, Gonzalez, Seibert, & Fair, 1997); see Fig. 1(a).
2. Catalyst particles sandwiched between corrugated sheets of wire gauze (Bart & Landschützer, 1996; Stringaro, 1991, 1995; Gelbein & Buchholz, 1991; Van Gulijk, 1998; Ellenberger & Krishna, 1999; Higler, Krishna, Ellenberger, & Taylor, 1999; Moritz & Hasse, 1999; Van Baten, Ellenberger, & Krishna, 2001; van Baten & Krishna, 2001); see Fig. 1(b). Such structures are being licensed by Sulzer, called KATAPAK-S, and by Koch-Glitsch, called KATAMAX (DeGarmo, Parulekar, & Pinjala, 1992). They consist of two pieces of rectangular crimped wire gauze sealed around the edge, thereby forming a pocket of the order of 1–5 cm wide between the two screens. These catalyst “sandwiches” are then bound together and placed inside the column.

An important claimed advantage of the structured criss-crossing catalyst sandwich structures shown in Fig. 1(b) over alternative configurations is with respect to radial distribution of liquid through the packed catalyst channels. Our earlier study, using both experiments and CFD techniques (Van Baten, Ellenberger, & Krishna, 2001), has shown that KATAPAK-S has excellent radial dispersion characteristics, which is a desirable feature in chemical reactors. The primary objective of the present communication is to extend our earlier work to the study of liquid phase and gas phase mass transfer within the sandwich structures. In view of the success of our earlier CFD approach to describe radial dispersion (Van Baten et al., 2001), we have extended this methodology to study mass transfer.

2. CFD model development

The computational space for the CFD simulations of the liquid flow in a single sandwich structure of KATAPAK-S is shown in Fig. 2; this corresponds to our experimental set up (see: http://ct-cr4.chem.uva.nl/strucsim/) used to study axial and radial dispersion. The sandwich exists of 16 triangular channels, with a total of 32 cross-overs. A single

---

* Corresponding author. Tel.: +31-20-525-7007; fax: +31-20-525-5604.
E-mail address: krishna@science.uva.nl (R. Krishna).

PII: S0009-2509(02)00026-X

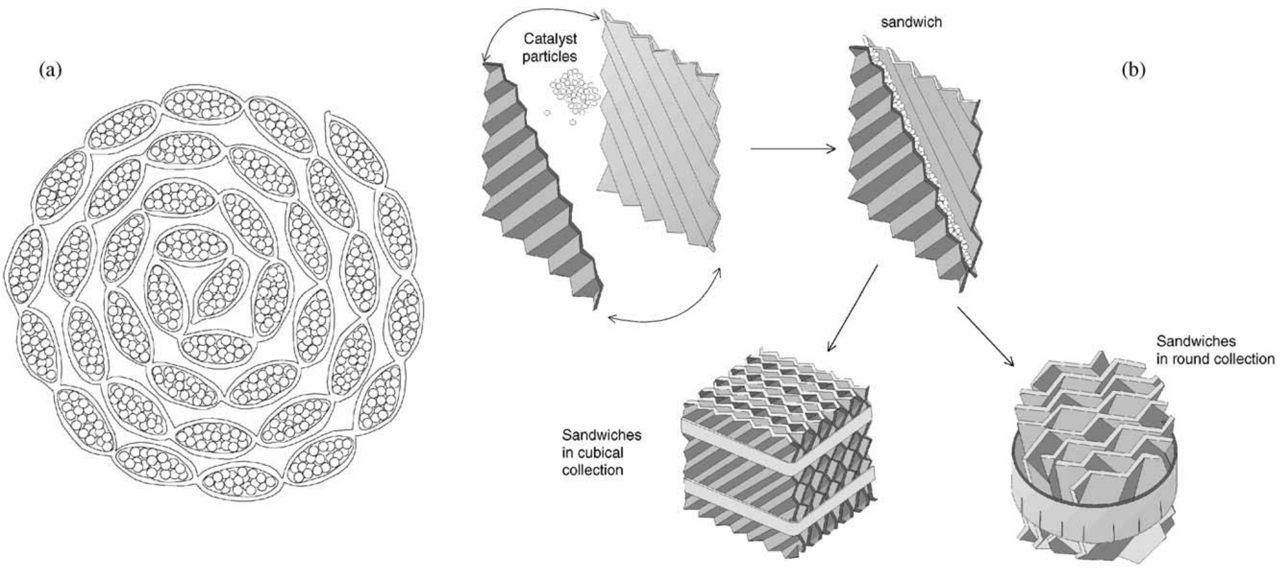

Fig. 1. (a) Catalyst bales licensed by Chemical Research and Licensing. (b) KATAPAK-S structure. Catalyst sandwiched between two corrugated wire gauze sheets, then joined together and sewn on all four sides into a sandwich “configuration”, arranged into a cubical collection or round collection.

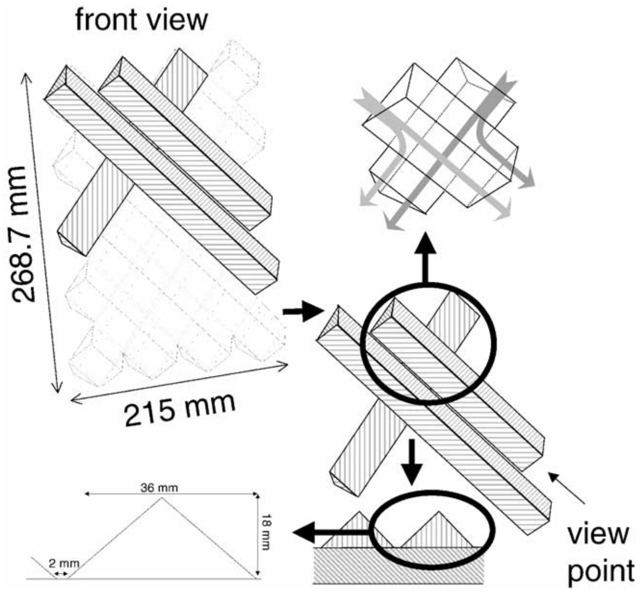

Fig. 2. Reconstruction of KATAPAK-S structure as a set of intersecting triangular tubes. A single sandwich consists of 16 triangular channels with 32 cross-overs. A single triangle is 36 mm wide and 18 mm high. A space of 2 mm is present between two adjoining triangular channels. The total number of grid cells used for either the open or packed channels, for gas and liquid mass transfer determinations, is 675584.

triangular channel has a base of 36 mm, and a height of 18 mm. There is a 2 mm gap between the bases of adjoining triangular channels. Inside such a sandwich, catalyst particles are present; the liquid flows inside these packed channels.

When taking two of these sandwiches and placing them together, the space in between the two sandwiches is geometrically nearly equal to the inside of a packed channel. The channels that will be formed by this space are referred to as the open channels; no catalyst particles are present in the open channels. The gas flows through these open channels.

In the CFD simulations, the liquid flows only through the packed channels and the gas flows only through the open (empty) channels. The interfacial area is determined purely by geometrical considerations. In order to study mass transfer, we introduce a tracer component on all the external surfaces of the (packed or unpacked) sandwich with a mass fraction $\omega = 1$, except on inlets and outlets. The liquid or gas flowing into the system does not contain the tracer component. The liquid or gas picks up tracer during its flow through the system. The amount of tracer that has been taken up by the liquid when the liquid leaves the system is then used to calculate a mass transfer coefficient for either liquid or gas phase.

The mass and momentum conservation equations for liquid flow through the packed channels are

$$\frac{\partial \varepsilon \rho_L}{\partial t} + \nabla \bullet (\rho_L \varepsilon \mathbf{u}_L) = 0, \tag{1}$$

$$\frac{\partial \rho_L \varepsilon \mathbf{u_L}}{\partial t} + \nabla \bullet (\rho_L \varepsilon \mathbf{u_L} \mathbf{u}_L - \mu_L \varepsilon (\nabla \mathbf{u}_L + (\nabla \mathbf{u}_L)^{\mathrm{T}})) = \varepsilon \mathbf{B} - \varepsilon \nabla p. \tag{2}$$

The liquid phase was taken to be water with $\rho_L = 998\ \mathrm{kg/m^3}$ and $\mu_L = 0.001$ Pa s. In the equation above, $\mathbf{B}$ is the body force resulting from the flow resistance caused by the catalyst particles present in the packed channels. This flow resistance is assumed to be isotropic, and with uniform porosity $\varepsilon = 0.37$. The Ergun equation (Bird, Stewart, & Lightfoot, 1960) has been used to formulate the resistance term $\mathbf{B}$ in Eq. (2). The particle size d_p in the equation above is taken to be 1.1 mm. The corresponding equations for gas flow through the open channels the above set of equations are obtained by taking the porosity $\varepsilon = 1$ and the flow resistance $\mathbf{B} = 0$.

Diffusion and convection of mass tracer is described by the following equation of continuity for either the packed or open channels:

$$\frac{\partial \varepsilon \rho_\alpha \omega}{\partial t} + \nabla \bullet (\rho_\alpha \varepsilon \omega u_\alpha) = \nabla \bullet (\rho_\alpha \varepsilon D_{\omega,\alpha} \nabla \omega), \tag{3}$$

where the subscript α refers to gas or liquid phase. Here, ω is the mass fraction of tracer in the liquid or gas phase. The diffusion coefficient D of tracer in water was taken 10^{-9} m^2/s, and the diffusion of tracer in the gas phase was taken 10^{-5} m^2/s. The porosity for the packed and open channels are respectively $\varepsilon = 0.37$ and 1. The liquid flow through the packed channels is in laminar. For the gas phase, the low-Reynolds k-epsilon model was invoked, with standard single-phase parameters.

Velocities are specified at the eight inlets of the structure. No-slip boundary conditions are applied to the walls. A Neumann boundary condition was applied to the velocities at the eight outlets.

For solving the above set of equations, a commercial CFD package CFX, version 4.2, was used with an algebraic multi-grid (AMG) solver. The simulations were run on a Silicon Graphics Power Challenge machine with 1 Gb RAM and a single 200 MHz R10K processor. Discretisation of the equations is performed using a finite volume method. Velocity vectors are treated as scalar equations, one equation for each of the three velocity components. All scalar variables are discretised and stored at the cell centres.

Velocities required at the cell faces are evaluated by applying improved Rhie–Chow interpolation (Rhie & Chow, 1983). Transport variables such as diffusion coefficients are evaluated and stored at the cell faces. The SIMPLEC (Van Doormal & Raithby, 1984) pressure correction method is applied. The equations are solved for steady state conditions. Differencing of the diffusion terms is performed by central differencing.

At steady state, the volumetric rate of transfer of tracer into phase α (α is G or L), $\phi_{\mathrm{tracer},\alpha}$, can be determined and the mass transfer coefficient k_α is obtained from

$$k_\alpha = \frac{\phi_{\mathrm{tracer},\alpha}}{A(\omega_{\mathrm{wall},\alpha} - \omega_{\mathrm{bulk},\alpha})}, \tag{4}$$

where A is the total external surface area of the sandwich structure in m^2; $\omega_{\mathrm{bulk},\alpha}$ is the mass fraction of tracer in the bulk leaving the system at the outlets under steady state. We can also determine the Sherwood number, Sh_α defined by

$$Sh_\alpha = \frac{k_\alpha d_H}{D_{\omega,\alpha}}, \tag{5}$$

where the hydraulic diameter of the system is denoted by d_H. The hydraulic diameters of the packed and open channels are the same and $d_H = 23.8$ mm.

3. Simulation results

For comparison purposes we also determined the mass transfer in an empty cylindrical tube of diameter 23.8 mm; see Fig. 3. Grid convergence was checked by varying the grid cell size near the wall. In our previous study (Van Baten et al., 2001) we found that an average cell size of about 2 mm within the structure was sufficient for solving the velocity profiles and determine the liquid dispersion characteristics. However, in the current problem, time and length scales near the wall are dominated by the process of molecular diffusion. Somewhat further from the wall, convection is the dominating process. Therefore, the required cell size near the wall for the current problem needs to be examined critically. Details of grid sizes and convergence for the liquid phase simulations are given on our web site: http://ctcr4.chem.uva.nl/walltracer/ and in our previous publication (van Baten & Krishna, 2001) which focussed on liquid phase mass transfer. For the empty tube running with liquid (not turbulent), it was found that 0.3 mm cells or finer need to be used at the wall to obtain grid convergence. For packed structures, a cell size at the wall of 0.01 mm was required. For the gas phase simulations (not packed, but possibly turbulent), it was found that the grid sizes used for the packed liquid phase simulations were required to be used, i.e. 0.01 mm at the wall.

The simulations for gas phase Sherwood number in empty circular tube are shown in Fig. 4 as a function of the gas phase Re number. For laminar flow conditions ($Re_G < 2100$) the CFD simulations show good agreement with the classical Graetz solution for mass transfer to laminar flow (Janssen & Warmoeskerken, 1991):

$$Sh = \begin{cases} 1.62\ Gz^{-1/3} & \text{for } Gz < 0.05, \\ 3.66 & \text{for } Gz > 0.1, \end{cases} \tag{6}$$

where the Graetz number is defined as

$$Gz = \frac{DL}{d_H^2 u}. \tag{7}$$

The agreement between the calculations using Eq. (6) and our CFD simulations shown in Fig. 4 for $Re < 2100$ lends

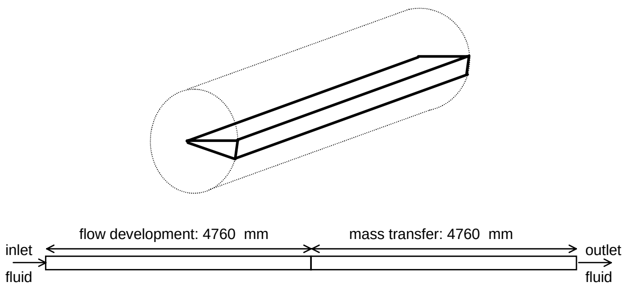

Fig. 3. Geometry used for determining mass transfer in an empty circular tube. To ensure fully developed flow a length equal to twenty times the tube diameter was used before the section at which tracer was injected.

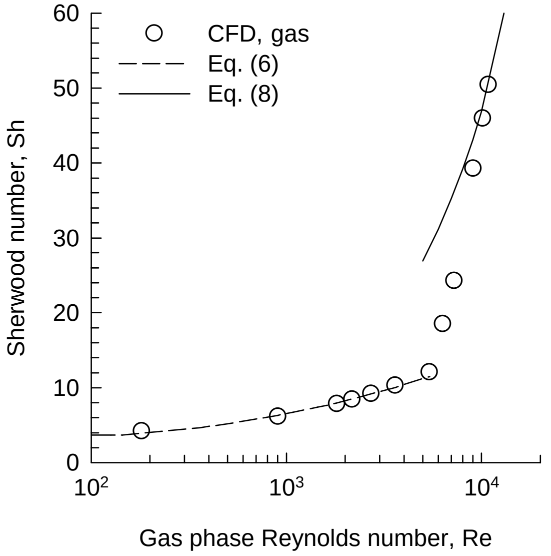

Fig. 4. Simulation results for gas phase mass transfer in an empty round tube: Sherwood numbers vs. gas velocity and *Re* number. Also plotted are the calculations using Eqs. (6) and (8).

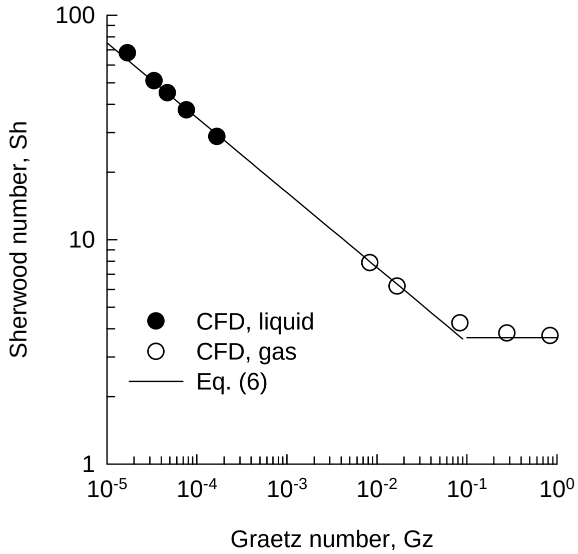

Fig. 5. Sherwood number for laminar flow of either liquid or gas through empty circular tube. The continuous line is drawn using Eq. (6).

confidence in our CFD procedure for mass transfer determination. For $2100 < Re_G < 6000$ the CFD simulations show a gradual increase in Sh_G values above those predicted by the Graetz solution, Eq. (6). Turbulence appears to kick in for $Re_G > 6000$ and Sh_G increases sharply and for $Re_G > 10000$ the Sh_G attain fully-developed turbulent mass transfer coefficient values corresponding the classical correlation (Janssen & Warmoeskerken, 1991):

$$Sh_G = 0.027 Re_G^{0.8} Sc_G^{0.33} \quad \text{for } Re_G > 10^4,\ Sc_G \geqslant 0.7. \tag{8}$$

The liquid phase Sherwood number determined from CFD simulations are compared with the Graetz solution (6) in Fig. 5 (this figure also includes the gas phase laminar flow data plotted in Fig. 4); again we note good agreement between the two in the laminar flow regime. Figs. 4 and 5 lend us confidence in our CFD procedure for estimating Sherwood numbers.

For the sandwich structure shown in Fig. 2, the CFD simulations of Sh_G for gas phase flow in the open channels are shown in Fig. 6 for a range of inlet gas velocities. For comparison purposes, the values obtained for a single circular tube are also shown in Fig. 6. Due to frequent criss-crossing at the intersections of the sandwich structure, the velocity profiles experience an "upheaval", leading to vastly improved mass transfer. At an inlet gas velocity of 2 m/s the value of Sh_G is four times that for an empty tube. There are no published experimental correlations for gas phase mass transfer in KATAPAK-S structures; Moritz and Hasse (1999) only present overall values of HETP for this structure. However, Subawalla et al. (1997) have presented detailed correlations for gas and liquid phase mass transfer in the catalytic bales structure portrayed in Fig. 1(a). Using the Subawalla et al. (1997) correlation we estimated the gas phase Sh_G using the geometrical parameters of KATAPAK-S; the resulting values are also shown in Fig. 6. There is good agreement between the CFD simulations and the correlation for bales. The conclusion to be drawn here is that cris-crossing of the channels of KATAPAK-S does not further enhance turbulent gas phase mass transfer as found in the bales structure.

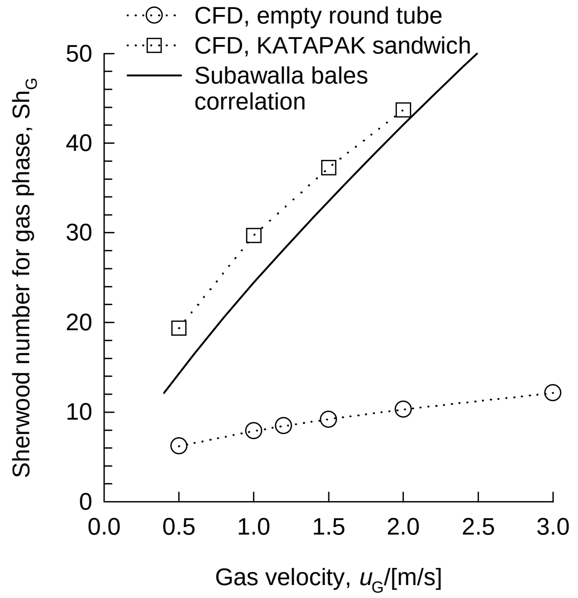

Fig. 6. Simulation results for gas phase mass transfer through the open channels of the sandwich structure shown in Fig. 2. Comparison with empty tube CFD simulations and with the Subawalla et al. (1997) correlation for catalytic bales.

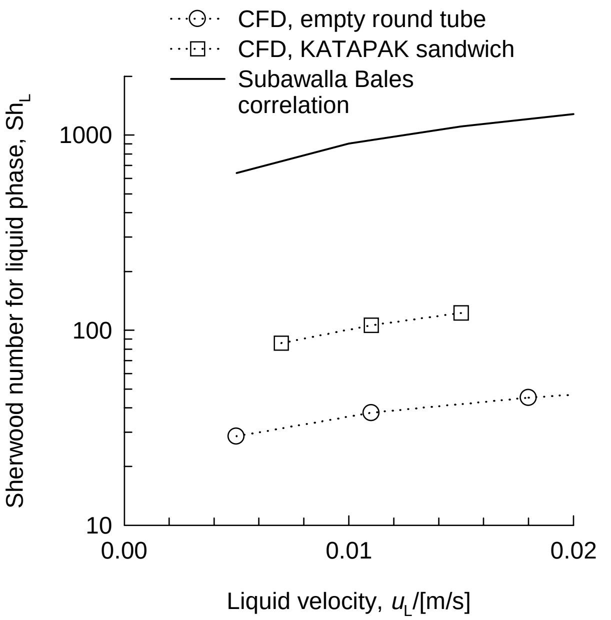

Fig. 7. Simulation results for liquid phase mass transfer through the packed channels of the sandwich structure shown in Fig. 2. Comparison with empty tube CFD simulations and with the Subawalla et al. (1997) correlation for catalytic bales.

For the sandwich structure, the CFD simulations of Sh_L for liquid phase flow in the packed channels are shown in Fig. 7 for a range of inlet liquid velocities. For comparison purposes the values obtained for a single circular (empty) tube are also shown in Fig. 7. As for the gas phase, the sandwich structure yields significantly improved mass transfer compared to that of an empty tube. Also plotted in Fig. 7 are the values of Sh_L obtained from the Subawalla et al. (1997) correlation for catalytic bales. Interestingly the values from the bales correlation of Subawalla yield Sh_L values that are about one order of magnitude higher than the values obtained from CFD simulations. Now, we do not expect the liquid phase Sh_L for bales to be lower than for KATPAK-S; on the contrary, frequent cris-crossing should yield a higher Sh_L for KATAPAK than for bales. The explanation for the discrepancy found in Fig. 7 lies in the basic assumption of the CFD simulations that the liquid phase flows only through the packed channels. In reality, some of the liquid seeps out of the packed channels and comes into direct contact with the gas phase. Our earlier study on liquid dispersion (Van Baten et al., 2001) provides direct evidence of bypassing of liquid through the open channels. Though bypassing of liquid leads to increased axial dispersion, that is undesirable, the liquid film flow in the open channels is rendered turbulent by direct contact with the gas phase. The mass transfer in the liquid phase is therefore much more efficient. We would also suggest that from a mass transfer point of view it is desirable to operate the KATAPAK-S structure at high liquid loads with considerable liquid by-passing; this would yield significantly improved liquid phase mass transfer coefficients.

4. Conclusions

The following conclusions can be drawn from the present study

(1) CFD simulations provide a convenient and powerful tool for studying mass transfer for walls to a flowing fluid phase. One important advantage of CFD simulation techniques is that complex geometries can be handled for which no empirical correlations are available.
(2) The CFD simulation results for gas phase mass transfer in an empty circular tube show a gradual increase when we move from laminar to turbulent flow conditions. The literature values for the limiting situations of laminar flow and fully developed turbulent flow are matched nicely. For liquid phase flow inside a circular tube only the laminar flow conditions were investigated; the *Sh* values correspond to those obtained from the classical Graetz solution.
(3) The values of *Sh* for gas and liquid phase flows in the sandwich structure (shown in Fig. 2) are significantly higher than for empty circular tubes. This is attributable to the frequent criss-crossing in the KATAPAK-S structures.
(4) The gas phase mass transfer in the sandwich structure agrees rather well with the Subawalla et al. (1997) correlation for catalytic bales.
(5) The liquid phase mass transfer in the sandwich structure, in contrast, are significantly lower than the values calculated by Subawalla et al. (1997) correlation for catalytic bales. The discrepancy is attributed to the fact that in practice, there will be liquid bypassing through the open channels; this liquid is in much more intense (turbulent) contact with the gas phase.
(6) We recommend operation of KATAPAK-S structure with a high degree of liquid bypassing in order to improve mass transfer. If the column is tall enough with several KATPAK-S elements placed one above the other the liquid bypassing has no detrimental effect at all because of liquid redistribution after each element in the vertical stack.

Notation

A	wall area, m^2
$\mathbf{B}$	body force, N/m^3
d	diameter, m
d_H	hydraulic diameter, m
D	diffusion coefficient of tracer, m^2/s
Gz	Graetz number, $DL/(d_H^2 u)$
k	mass transfer coefficient, m/s
L	length, m
n	normal
p	pressure, Pa
r	radius, m

Re	Reynolds number, $\rho u d_H/\mu$
Sc	Schmidt number, $\mu/(\rho D)$
Sh	Sherwood number, $k d_H/D$
t	time, s
$\mathbf{u}$	velocity vector, m/s
u	interstitial velocity, m/s

Greek letters

ε	porosity of packing, dimensionless
ϕ_{tracer}	flux of tracer, m^3/s
ρ	density, kg/m^3
μ	viscosity, Pa s
ω	tracer concentration, dimensionless

Subscripts

α	phase, either liquid (L) or gas (G)
bulk	away from the wall, in the bulk
G	gas phase
H	hydraulic
L	liquid phase
p	particle
wall	at the wall

Acknowledgements

Financial assistance from The Netherlands Organization for Scientific Research (NWO) in the form of a "programmasubsidie" for development of novel concepts in reactive separations is gratefully acknowledged.

References

Bart, H.-J., & Landschützer, H. (1996). Heterogene Reaktivdestillation mit axialer Rückvermischung. *Chemie Ingenieur Technik*, *68*, 944–946.

Van Baten, J. M., Ellenberger, J., & Krishna, R. (2001). Radial and axial dispersion of the liquid phase within a KATAPAK-S® structure: Experiments vs. CFD simulations. *Chemical Engineering Science*, *56*, 813–821.

van Baten, J. M., & Krishna, R. (2001). Liquid phase mass transfer within KATAPAK-S® structures studied using CFD simulations. *Catalysis Today*, *69*, 371–377.

Bird, R. B., Stewart, W. E., & Lightfoot, E. N. (1960). *Transport phenomena*. New York: Wiley.

DeGarmo, J. L., Parulekar, V. N., & Pinjala, V. (1992). Consider reactive distillation. *Chemical Engineering Progress*, *3*, 43–50.

Van Doormal, J., & Raithby, G. D. (1984). Enhancement of the SIMPLE method for predicting incompressible flows. *Numerical Heat Transfer*, *7*, 147–163.

Ellenberger, J., & Krishna, R. (1999). Counter-current operation of structured catalytically packed distillation columns: pressure drop, hold-up and mixing. *Chemical Engineering Science*, *54*, 1339–1345.

Gelbein, A. P., & Buchholz, M. (1991). *Process and structure for effecting catalytic reactions in distillation structure*. US Patent No. 5073236.

Van Gulijk, C. (1998). Using computational fluid dynamics to calculate transversal dispersion in a structured packed bed. *Computers and Chemical Engineering*, *22*, S767–S770.

Higler, A. P., Krishna, R., Ellenberger, J., & Taylor, R. (1999). Counter-current operation of a structured catalytically packed bed reactor: Liquid phase mixing and mass transfer. *Chemical Engineering Science*, *54*, 5145–5152.

Janssen, L. P. B. M., & Warmoeskerken, M. M. C. G. (1991). *Transport phenomena data companion* (2nd ed.). Delft, Holland: Delftse Uitgevers Maatschappij.

Johnson, K. H., & Dallas, A. B. (1994). *Catalytic distillation structure*. US Patent No. 5348710.

Moritz, P., & Hasse, H. (1999). Fluid dynamics in reactive distillation packing Katapak®-S. *Chemical Engineering Science*, *54*, 1367–1374.

Rhie, C. M., & Chow, W. L. (1983). Numerical study of the turbulent flow past an airfoil with trailing edge separation. *AIAA Journal*, *21*, 1525–1532.

Smith Jr., L. A. (1985). *Catalytic distillation process and catalyst*. European Patent No. 008860B1.

Stringaro, J. P. (1991). *Reactor including a catalyst body for performing a heterogeneous reaction*. European Patent No. 433222A1.

Stringaro, J. P. (1995). *Catalyzing fixed bed reactor*. US Patent No. 5470542.

Subawalla, H., Gonzalez, J. C., Seibert, A. F., & Fair, J. R. (1997). Capacity and efficiency of reactive distillation bale packing: Modeling and experimental validation. *Industrial and Engineering Chemistry Research*, *36*, 3821–3832.

Taylor, R., & Krishna, R. (2000). Modelling reactive distillation. *Chemical Engineering Science*, *55*, 5183–5229.